

AD-A252 800



AEROSPACE REPORT NO.
TR-0091(6940-07)-1

2

Vibrational Relaxation of H₂O by H₂, HCl, and H₂O at 295K

Prepared by

P. F. ZITTEL and D. E. MASTURZO
Space and Environment Technology Center
Technology Operations

16 June 1992

DTIC
ELECTE
JUL 14 1992
S B D

Prepared for

SPACE SYSTEMS DIVISION
AIR FORCE SYSTEMS COMMAND
Los Angeles Air Force Base
P. O. Box 92960
Los Angeles, CA 90009-2960

Contract No. F04701-88-C-0089

Engineering and Technology Group

THE AEROSPACE CORPORATION
El Segundo, California



APPROVED FOR PUBLIC RELEASE;
DISTRIBUTION UNLIMITED

92-18430

92 7 13 155

This report was submitted by The Aerospace Corporation, El Segundo, CA 90245-4691, under Contract No. F04701-88-C-0089 with the Space Systems Division, P. O. Box 92960, Los Angeles, CA 90009-2960. It was reviewed and approved for The Aerospace Corporation by A. B. Christensen, Principal Director, Space and Environment Technology Center. Major Michael Goodman was the project officer for the Mission-Oriented Investigation and Experimentation (MOIE) program.

This report has been reviewed by the Public Affairs Office (PAS) and is releasable to the National Technical Information Service (NTIS). At NTIS, it will be available to the general public, including foreign nationals.

This technical report has been reviewed and is approved for publication. Publication of this report does not constitute Air Force approval of the report's findings or conclusions. It is published only for the exchange and stimulation of ideas.



MARTIN K. WILLIAMS, Capt, USAF
Mgr, Space Systems Integration
DCS for Program Management



MICHAEL J. GOODMAN, Major, USAF
Sensor Development Program Manager
Brilliant Eyes SPO

REPORT DOCUMENTATION PAGE

1a. REPORT SECURITY CLASSIFICATION Unclassified			1b. RESTRICTIVE MARKINGS		
2a. SECURITY CLASSIFICATION AUTHORITY			3. DISTRIBUTION/AVAILABILITY OF REPORT Approved for public release; distribution unlimited		
2b. DECLASSIFICATION/DOWNGRADING SCHEDULE					
4. PERFORMING ORGANIZATION REPORT NUMBER(S) TR-0091(6940-07)-1			5. MONITORING ORGANIZATION REPORT NUMBER(S) SSD-TR-92-14		
6a. NAME OF PERFORMING ORGANIZATION The Aerospace Corporation Technology Operations		6b. OFFICE SYMBOL (If applicable)	7a. NAME OF MONITORING ORGANIZATION Space Systems Division		
6c. ADDRESS (City, State, and ZIP Code) El Segundo, CA 90245-4691			7b. ADDRESS (City, State, and ZIP Code) Los Angeles Air Force Base Los Angeles, CA 90009-2960		
8a. NAME OF FUNDING/SPONSORING ORGANIZATION		8b. OFFICE SYMBOL (If applicable)	9. PROCUREMENT INSTRUMENT IDENTIFICATION NUMBER F04701-88-C-0089		
8c. ADDRESS (City, State, and ZIP Code)			10. SOURCE OF FUNDING NUMBERS		
			PROGRAM ELEMENT NO.	PROJECT NO.	TASK NO.
			WORK UNIT ACCESSION NO.		
11. TITLE (Include Security Classification) Vibrational Relaxation of H ₂ O by H ₂ , HCl, and H ₂ O at 295K					
12. PERSONAL AUTHOR(S) Zittel, P. F. and Masturzo, D. E.					
13a. TYPE OF REPORT		13b. TIME COVERED FROM _____ TO _____		14. DATE OF REPORT (Year, Month, Day) 1992 June 16	
				15. PAGE COUNT 26	
16. SUPPLEMENTARY NOTATION					
17. COSATI CODES			18. SUBJECT TERMS (Continue on reverse if necessary and identify by block number)		
FIELD	GROUP	SUB-GROUP	Vibrational Relaxation Water Vapor		
19. ABSTRACT (Continue on reverse if necessary and identify by block number)					
<p>A laser-induced fluorescence method has been used to measure rate constants for vibrational relaxation of the equilibrated ν_1 and ν_3 stretching level reservoir, the $2\nu_2$ bending overtone level, and the ν_2 bending level of H₂O by H₂ and HCl at 295K. The rate constants for relaxation by H₂ were found to be 8.0 ± 1.1, 29 ± 4, and $13 \pm 2 \times 10^{-13} \text{ cm}^3 \text{ molecule}^{-1} \text{ s}^{-1}$, respectively. For relaxation by HCl, the rate constants were 8.4 ± 1.2, 47 ± 7, and $24 \pm 4 \times 10^{-12} \text{ cm}^3 \text{ molecule}^{-1} \text{ s}^{-1}$, respectively. Relaxation by <i>intermolecular</i> V→V transfer was experimentally determined to account for < 8% of the rate constant for relaxation of the H₂O stretching levels by HCl, and was estimated to contribute < 16% of the rate constant for relaxation of the bending overtone level. For both collision partners, the H₂O stretching levels were relaxed predominantly to the $2\nu_2$ level, and the $2\nu_2$ level was relaxed predominantly to ν_2.</p> <p>Following direct laser excitation, the rate constant for relaxation of the equilibrated $\nu_1 + \nu_2$ and $\nu_3 + \nu_2$ combination vibrational levels of H₂O by H₂O was measured to be $1.6 \pm 0.2 \times 10^{-10} \text{ cm}^3 \text{ molecule}^{-1} \text{ s}^{-1}$. Direct relaxation to the ν_1 and ν_3 fundamental levels was experimentally determined to account for < 40% of the relaxation rate constant.</p>					
20. DISTRIBUTION/AVAILABILITY OF ABSTRACT <input checked="" type="checkbox"/> UNCLASSIFIED/UNLIMITED <input type="checkbox"/> SAME AS RPT. <input type="checkbox"/> DTIC USERS			21. ABSTRACT SECURITY CLASSIFICATION Unclassified		
22a. NAME OF RESPONSIBLE INDIVIDUAL			22b. TELEPHONE (Include Area Code)		22c. OFFICE SYMBOL

CONTENTS

I.	INTRODUCTION	5
II.	EXPERIMENTAL	7
III.	RESULTS AND ANALYSIS	9
	A. RELAXATION OF H ₂ O BY H ₂	9
	B. RELAXATION OF H ₂ O BY HCl	15
	C. RELAXATION OF THE $\nu_1 + \nu_2$ AND $\nu_3 + \nu_2$ LEVELS OF H ₂ O	18
IV.	DISCUSSION	23
	REFERENCES	27

Accession For	
NTIS GRA&I	<input checked="" type="checkbox"/>
DTIC TAB	<input type="checkbox"/>
Unannounced	<input type="checkbox"/>
Justification _____	
By _____	
Distribution/ _____	
Availability Codes	
Dist A-1	Avail and/or Special

FIGURES

1.	H ₂ O Vibrational Relaxation in H ₂ O/H ₂ Mixtures	11
2.	H ₂ O Vibrational Relaxation in Mixtures of HCl in an H ₂ O/Ar Carrier Gas	16
3.	H ₂ O Vibrational Relaxation in H ₂ O/Ar Mixtures	20

TABLES

1.	Rate Constants for Vibrational Relaxation of H ₂ O at 295K	12
2.	Branching Ratios for Vibrational Relaxation of H ₂ O at 295K	14

I. INTRODUCTION

Vibrational relaxation of water vapor has been studied by various techniques including laser-induced fluorescence (LIF),¹⁻⁴ laser pump/probe,⁵ E→V transfer from electronically excited halogen atoms,^{6,7} ultrasonic absorption and dispersion,^{8,9} shock waves,¹⁰ and H₂O laser gain.¹¹ LIF measurements have provided detailed information on relaxation of and among the ν_1 , ν_2 , $2\nu_2$, and ν_3 vibrational levels. An unusual picture has emerged of very efficient V→T,R relaxation of the bending vibrational levels and less efficient V→V relaxation between bending and stretching modes. V→T,R self-relaxation of the lowest energy (ν_2 bending) level has been studied over a broad temperature range by LIF, ultrasonic, and shock tube methods. The observed negative temperature dependence of the relaxation probability below ~1000K is attributed to the effect of strong hydrogen bonding forces. Theoretical models¹²⁻¹⁴ suggest that attractive forces and rotational motion are critical factors in the vibrational relaxation of H₂O.

In the present study, rate constants are measured for relaxation of the equilibrated ν_1 and ν_3 stretching levels, the $2\nu_2$ bending overtone level, and the ν_2 bending level of water by H₂ and HCl. The dominant paths for relaxation of the stretching and bending overtone levels are determined from the total relaxation rate constants and fluorescence intensity measurements. Relaxation by the hydrogen bonding molecule HCl is found to be very similar to H₂O self-relaxation in both the magnitude of the total relaxation rate constants and the relative unimportance of intermolecular V→V transfer. Self-relaxation of the stretch-plus-bend combination levels of H₂O is also investigated. Relaxation is found to be extremely efficient and dominated by V→V transfer from stretching to bending modes.

II. EXPERIMENTAL

The experimental apparatus used in this study has been described in detail elsewhere.⁴ A brief description with details relevant to the present work is given here. The experiments were conducted in a quartz flow tube at 295K at pressures of 1-42 Torr. A flow of H₂O mixed in a carrier gas (Ar or H₂) was delivered to the flow tube from a large reservoir bulb. The adjustable mole fraction of H₂O was determined by the vapor pressure of a pool of liquid water in the reservoir bulb and the total bulb pressure, which was maintained by a servo-controlled flow of the carrier gas bubbled into the reservoir through the pool of water. Very small mole fractions of H₂O in the carrier gas were achieved by mixing the calibrated reservoir flow with a calibrated flow of pure carrier gas in the flow tube. For measurements of relaxation by HCl, a calibrated flow of a fixed concentration of H₂O in Ar from the reservoir bulb (i.e., [H₂O]/[Ar]=0.0794) was combined in the flow tube with an adjustable, calibrated flow of pure HCl to achieve a range of HCl mole fractions. Argon (Air Products research grade, >99.9995%), H₂ (Air Products ultra high purity grade, >99.995%), HCl (Matheson semiconductor grade, >99.995%) and water (distilled, deionized, and degassed by freeze-pump-thaw cycles) were used without further purification.

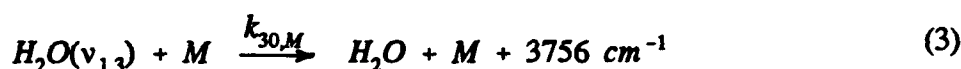
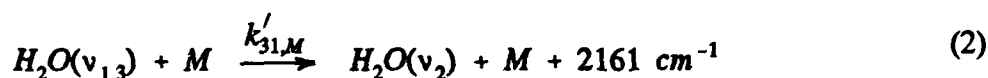
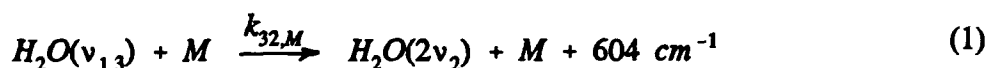
Laser-induced fluorescence experiments were conducted at an observation cross in the flow tube, where H₂O molecules were excited by a Nd:YAG-pumped, frequency difference laser system (5-6 ns pulsewidth, 2.5 mJ/pulse at 2.6 μ m, 5.0 mJ/pulse at 1.9 μ m). Vibrational fluorescence was imaged on a fast Cu:Ge detector (\sim 100 ns RC time), and the resulting signal was amplified and signal-averaged. In measurements of relaxation by H₂ and HCl, the H₂O was initially excited to the ν_3 vibrational level with the laser tuned to $\lambda=2.5946$ μ m to maximize coincidence with the $JK_aK_c \rightarrow J'K'_aK'_c = 321 \rightarrow 422, 404 \rightarrow 505, \text{ and } 312 \rightarrow 413$ rotational transitions of the absorption band.¹⁵ In measurements of relaxation by H₂, fluorescence at 2.7 μ m from the H₂O ν_3 (and to a much lesser extent ν_1) vibrational level was isolated by a combination of a long wavelength pass interference filter with a half-power point of 2.67 μ m and an IR grade quartz flat acting as a short wavelength pass filter with a half-power point of 4.1 μ m. In measurements of relaxation by HCl, the H₂O 2.7 μ m fluorescence was isolated by a bandpass interference filter with half-power points of 2.67 and 2.89 μ m. Possible HCl($v=1 \rightarrow 0$) fluorescence was isolated by a combination of a long wavelength pass filter with a half-power point of 3.24 μ m and an IR grade quartz flat acting as a short wavelength pass filter. In all mixtures, fluorescence on the $2\nu_2 \rightarrow \nu_2$ and $\nu_2 \rightarrow 0$ transitions of H₂O at 6.3 μ m was isolated by a combination of a long wavelength pass filter with half-power point at 5.05 μ m and a MgF₂ flat acting as a short wavelength pass filter with half-power point at 8.5 μ m. The 6.3 μ m fluorescence was recorded with a cold gas filter (8 cm path, 19 Torr H₂O) in the optical path to pass only $2\nu_2 \rightarrow \nu_2$ fluorescence, as well as with the filter evacuated to pass both $2\nu_2 \rightarrow \nu_2$ and $\nu_2 \rightarrow 0$ fluorescence.

In measurements of the relaxation of the combination vibrational levels, H_2O was initially pumped to the $\nu_2 + \nu_3$ level with the laser tuned to $\lambda = 1.8997 \mu\text{m}$ to coincide with the $\text{JK}_a\text{K}_c \rightarrow \text{J}'\text{K}'_a\text{K}'_c = 303 \rightarrow 202$ rotational transition of the ν band.¹⁶ The populations of the $\nu_2 + \nu_3$ combination level and the ν_3 fundamental level were monitored by observing $2.7 \mu\text{m}$ fluorescence on the $\nu_3 + \nu_2 \rightarrow \nu_2$ hot band and $\nu_3 \rightarrow 0$ fundamental band, respectively. Both bands were isolated from other fluorescence by a combination of a long wavelength pass filter with a half-power point at $2.60 \mu\text{m}$ and a quartz flat acting as a short wavelength pass filter. The two bands were separated from each other by using a cold gas filter in the optical path.

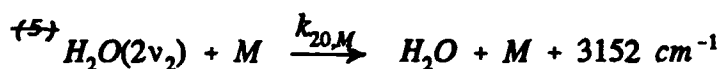
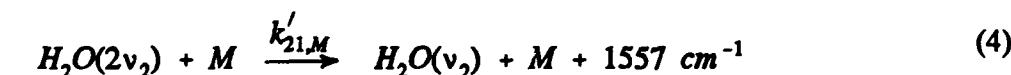
III. RESULTS AND ANALYSIS

A. RELAXATION OF H₂O BY H₂

The general kinetic scheme for relaxation of the fundamental stretching and lower energy bending vibrational levels of H₂O has been described in detail elsewhere.^{1,4} We use the previous notation for numbering vibrational levels and kinetic rate constants with some additions for new levels and relaxation processes. It has been demonstrated experimentally for H₂O self-relaxation,¹ and suggested by theoretical calculations for relaxation by Ar,¹⁷ that relaxation between the nearly resonant ν_1 and ν_3 stretching levels of H₂O is approximately gas kinetic and much faster than relaxation out of the stretching levels. After an initial rapid equilibration, the ν_1 and ν_3 levels relax together as a single reservoir which we designate by the notation $\nu_{1,3}$. The processes for V→T,R and intramolecular V→V relaxation of the stretching reservoir by collision partner M (=H₂ in this case) are given by



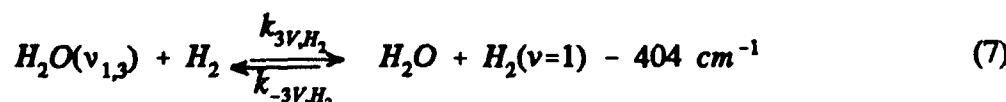
The energy defects are given for the ν_3 level and are 99 cm⁻¹ smaller for the ν_1 level.¹⁸ The rate constants for relaxation of the stretching level reservoir are the Boltzmann-weighted averages of the rate constants for the individual ν_1 and ν_3 levels. For relaxation of the bending overtone level, the relaxation processes are



For relaxation of the bending fundamental level, the relaxation process is



Relaxation by H₂ may also involve the intermolecular V→V process



The total relaxation rate constants $k_{3,M}$, $k_{2,M}$, and $k_{1,M}$ are defined as the sum of the rate

constants for all relaxation paths from the $\nu_{1,3}$ reservoir, the $2\nu_2$ level, and the ν_2 level, respectively.

In the absence of intermolecular V→V exchange between H₂O and H₂, the solution to the differential equations implied by Eqs. (1) through (6) is straightforward.^{1,4} The population of the $\nu_{1,3}$ stretching reservoir (2.7 μm , $\nu_{1,3}\rightarrow 0$ fluorescence) decays as a single exponential with the total $\nu_{1,3}$ reservoir relaxation rate constant k_{3,H_2} . The population of the $2\nu_2$ level (6.3 μm , $2\nu_2\rightarrow\nu_2$ fluorescence) follows a rise/fall double exponential with one relaxation rate constant identical to k_{3,H_2} and the other equal to the total $2\nu_2$ level relaxation rate constant k_{2,H_2} . Finally, the population of the ν_2 level (6.3 μm , $\nu_2\rightarrow 0$ fluorescence) follows a triple exponential with two of the relaxation rate constants identical to k_{3,H_2} and k_{2,H_2} and the third equal to the ν_2 level V→T,R relaxation rate constant k_{1,H_2} ($\equiv k_{10,H_2}$). Equivalently, one may extract k_{1,H_2} from the total 6.3 μm fluorescence ($2\nu_2\rightarrow\nu_2$ plus $\nu_2\rightarrow 0$), which is a triple exponential with the same relaxation rate constants as the $\nu_2\rightarrow 0$ fluorescence.

Relaxation rate constants were measured for the $\nu_{1,3}$ stretching level reservoir, the $2\nu_2$ level, and the ν_2 level of H₂O as a function of the mole fraction of H₂O in H₂. The decay of the 2.7 μm , $\nu_{1,3}\rightarrow 0$ fluorescence was a simple single exponential for all H₂O mole fractions. Small corrections for diffusion of vibrationally excited H₂O out of the detector field of view⁴ were made to the experimental relaxation times (i.e., < 3.5% in the worst case). The observed rate constants (i.e., $1/P_{\text{total}}\tau_{\text{relaxation}}$) for relaxation of the $\nu_{1,3}$ reservoir are shown in Figure 1 as a function of H₂O mole fraction. No evidence was seen in the temporal shape or amplitude of the fluorescence signals for intermolecular V→V equilibration between H₂O and H₂ prior to relaxation of the stretching levels. A rate constant reported¹⁹ for vibrational relaxation of H₂($v=1$) by H₂O implies, by detailed balance, an upper limit on k_{3V,H_2} in Eq. (7). The limit is a factor of ~ 60 smaller than the total relaxation rate constant k_{3,H_2} measured here in the limit of infinite dilution of H₂O. Thus, the intermolecular V→V process makes a negligible contribution to relaxation of H₂O($\nu_{1,3}$) by H₂. The 6.3 μm , $2\nu_2\rightarrow\nu_2$ fluorescence observed through a cold gas filter was fit by a rise/fall double exponential and gave rate constants for the fluorescence fall which were identical to those obtained from the 2.7 μm fluorescence decay and rate constants for the rise which are shown in Figure 1. Finally, the relaxation rate constants for the ν_2 level in Figure 1 were obtained by fitting a triple exponential to the total 6.3 μm fluorescence (i.e., $2\nu_2\rightarrow\nu_2$ plus $\nu_2\rightarrow 0$) while fixing two of the relaxation times at the times derived from the $\nu_{1,3}\rightarrow 0$ and $2\nu_2\rightarrow\nu_2$ fluorescence signals for the same gas sample. The intercepts of the least-squares linear fits to the data for the different vibrational levels give the total relaxation rate constants k_{3,H_2} , k_{2,H_2} and k_{1,H_2} for relaxation of H₂O by H₂, which are listed in Table 1.

In addition to the total relaxation rate constants, some information may also be deduced about the importance of competing, path-specific rate constants for relaxation of the stretching reservoir and bending overtone level of H₂O by H₂. The relative amplitudes of the 6.3 μm ,

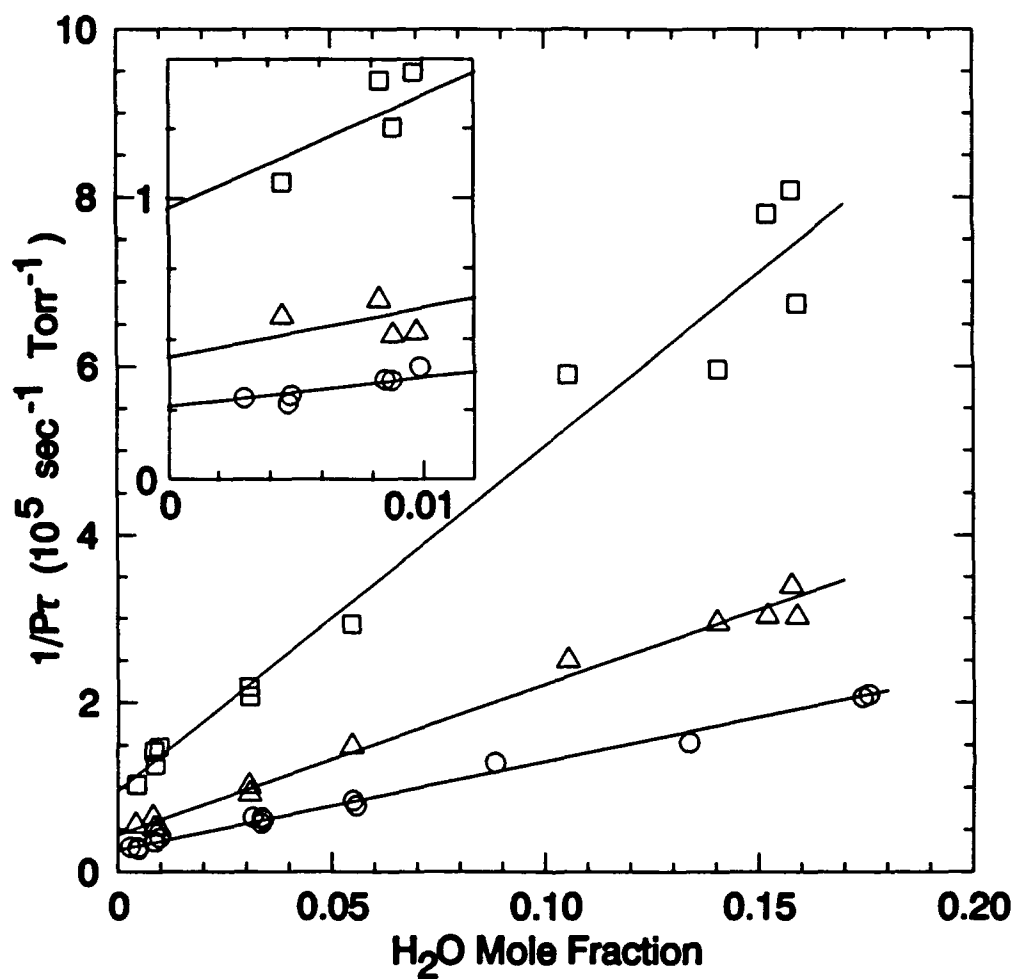


Figure 1. H₂O Vibrational Relaxation in H₂O/H₂ Mixtures. The observed relaxation rate constants are for the $\nu_{1,3}$ reservoir (\circ), ν_2 level (Δ), and $2\nu_2$ level (\square). The experimental uncertainty in the ordinate of a data point is $\pm 10\%$. The lines are error-weighted, least-squares linear fits to the data.

Table 1. Rate Constants for Vibrational Relaxation of H₂O at 295K.

Vibrational level i	Collision partner M	$k_{i,M}^a$ (cm ³ molecule ⁻¹ s ⁻¹)	P ^b
$\nu_{1,3}^c$	H ₂	$8.0 \pm 1.1 \times 10^{-13}$	1.6×10^{-3}
$2\nu_2$	H ₂	$2.9 \pm 0.4 \times 10^{-12}$	6.1×10^{-3}
ν_2	H ₂	$1.3 \pm 0.2 \times 10^{-12}$	2.7×10^{-3}
$\nu_{1,3}^c$	HCl	$8.4 \pm 1.2 \times 10^{-12}$	0.040
$2\nu_2$	HCl	$4.7 \pm 0.7 \times 10^{-11}$	0.22
ν_2	HCl	$2.4 \pm 0.4 \times 10^{-11}$	0.12
$\nu_{1,3} + \nu_2$	H ₂ O	$1.6 \pm 0.2 \times 10^{-10}$	0.79
$\nu_{1,3} + \nu_2$	Ar	$< 6 \times 10^{-13}$	$< 3 \times 10^{-3}$

^a Total relaxation rate constant for level i by collision partner M. The uncertainty is $\pm 2\sigma$ determined from the least-squares linear fits to the experimental data.

^b Relaxation probability, $P = k_{i,M}/k_{gk,M}$, where $k_{gk,M}$ is the gas kinetic collision rate constant calculated using collision diameters of 2.8, 2.96, 3.3, and 3.4 Å for H₂O, H₂, HCl, and Ar, respectively.

^c The notation $\nu_{1,3}$ is used to indicate that the ν_1 and ν_3 levels are in rapid equilibrium and relax together as a single reservoir. The same is presumed to be true for the $\nu_1 + \nu_2$ and $\nu_3 + \nu_2$ combination levels where the reservoir of equilibrated levels is designated $\nu_{1,3} + \nu_2$.

$2\nu_2 \rightarrow \nu_2$ and $\nu_2 \rightarrow 0$ fluorescence signals may be combined with the radiative lifetimes on the two transitions and the measured total relaxation rate constants to experimentally define the quantities C_{1,H_2} ($\equiv k'_{21,H_2}$) and Z_{H_2} ($\equiv k'_{31,H_2}/k_{32,H_2}$). The definitions of C_1 and Z in terms of experimental parameters are discussed in detail elsewhere.⁴ The values derived for relaxation of H_2O by H_2 were $C_{1,H_2} = 2.3 \pm 0.6 \times 10^{-12} \text{ cm}^3 \text{ molecule}^{-1} \text{ sec}^{-1}$ from a plot of C_1 vs. H_2O mole fraction and $Z_{H_2} = 0.15 \pm 0.15$ in the limit of infinite dilution of H_2O . The value for C_{1,H_2} gives the expected result that relaxation of the $2\nu_2$ level by H_2 is dominated by the single quantum $V \rightarrow T, R$ process (i.e., $k'_{21,H_2}/k_{2,H_2} = 0.8 \pm 0.2$). The value for Z_{H_2} determines that $V \rightarrow V$ relaxation of the stretching reservoir to the ν_2 level is much less efficient than relaxation to the $2\nu_2$ level (i.e., $k'_{31,H_2}/k_{32,H_2} = 0.15 \pm 0.15$). In addition, if it is assumed that the rate constant k_{30,H_2} for $V \rightarrow \bar{T}, R$ relaxation of the $\nu_{1,3}$ reservoir to the ground state is smaller than the rate constant k'_{31,H_2} for the much less exothermic $V \rightarrow V$ relaxation to the ν_2 level, then the experimental value of Z_{H_2} also implies that the stretching reservoir is relaxed *predominantly* to the $2\nu_2$ level (i.e., $k_{32,H_2}/k_{3,H_2} > 0.6$). The conclusions concerning path-specific rate constants are summarized in Table 2.

The H_2O/H_2 mixture results also determine rate constants and branching ratios for H_2O self-relaxation. The slopes and intercepts of the fits in Figure 1 give values of 5.5 ± 0.6 , 12.8 ± 1.3 , and $3.2 \pm 0.3 \times 10^{-11} \text{ cm}^3 \text{ molecule}^{-1} \text{ s}^{-1}$ for the total self-relaxation rate constants k_{1,H_2O} , k_{2,H_2O} , and k_{3,H_2O} , respectively. The results are identical ($\pm 7\%$) to those measured previously in mixtures of H_2O with He and Ar.⁴ The parameters⁴ C_{1,H_2O} ($\equiv 2k_{21,H_2O} + k'_{21,H_2O}$) and Z_{H_2O} ($\equiv [2k_{31,H_2O} + k'_{31,H_2O}]/k_{32,H_2O}$) were also determined experimentally to be $7.7 \pm 1.7 \times 10^{-11} \text{ cm}^3 \text{ molecule}^{-1} \text{ s}^{-1}$ and 0.32 ± 0.16 , respectively. The results determine the branching ratios for H_2O self-relaxation listed in Table 2 along with previous measurements.^{1,4} The H_2O self-relaxation processes are defined by Eqs. (1) through (6) with $M=H_2O$ and by the additional intermolecular $V \rightarrow V$ processes

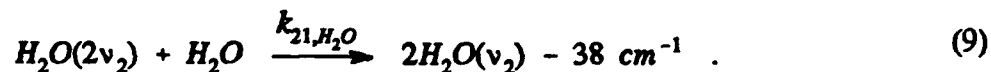
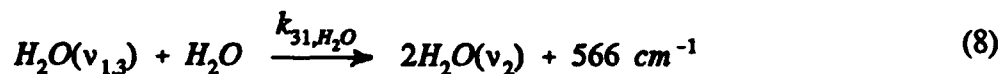


Table 2. Branching Ratios for Vibrational Relaxation of H₂O at 295K.

	M		
	H ₂	HCl	H ₂ O
$k_{3V,M}/k_{3,M}$	<0.016 ^a	<0.08	-
$(2k_{31,H_2O} + k'_{31,H_2O})/k_{32,H_2O}$	-	-	0.32 ± 0.16 , ^b 0.22 ± 0.14 ^c
$k'_{31,M}/k_{32,M}$	0.15 ± 0.15	0.10 ± 0.10	-
$k_{32,M}/k_{3,M}$	>0.6 ^d	>0.7 ^d	>0.4, ^{b,d} >0.4, ^{c,d} >0.3 ^{d,e}
$k_{2V,M}/k_{2,M}$	-	<0.16	-
$(2k_{21,H_2O} + k'_{21,H_2O})/k_{2,H_2O}$	-	-	0.60 ± 0.20 , ^b 0.63 ± 0.25 ^c
$k_{21,H_2O}/k_{2,H_2O}$	-	-	<0.3, ^{b,f} <0.3 ^{c,f}
$k'_{21,M}/k_{2,M}$	0.8 ± 0.2	0.8 ± 0.2	>0.35, ^{b,f} >0.31, ^{c,f} >0.5 ^{f,g}
$(k'_{73,H_2O} + k_{73,H_2O})/k_{7,H_2O}$	-	-	<0.4

^a Upper limit on k_{3V,H_2} from Ref. 19.

^b From H₂O/H₂ mixture^c results in this study.

^c From Ref. 4.

^d Derived with assumption about the relative magnitude of k_{30} . See text and Ref. 4.

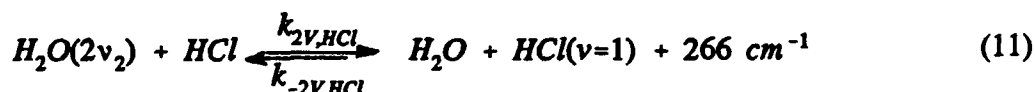
^e Calculated here from results for H₂¹⁸O in Ref. 1.

^f Derived with assumption about the relative magnitudes of k'_{21} and k_{10} . See Ref. 4.

^g From Ref. 1 for H₂¹⁸O.

B. RELAXATION OF H₂O BY HCl

The V→T,R and intramolecular V→V processes for relaxation of H₂O by HCl are described by Eqs. (1) through (6) with M=HCl. In addition one must consider the intermolecular V→V processes



where the energy defects are given for H³⁵Cl. It is demonstrated experimentally that the intermolecular V→V processes make minor contributions to relaxation of the H₂O stretching reservoir and bending overtone level (see below). Consequently, the relaxation of H₂O by HCl is described essentially by Eqs. (1) through (6).

Relaxation of H₂O by HCl was studied in mixtures of HCl in an H₂O/Ar carrier gas of fixed composition (i.e., [H₂O]/[Ar]=0.0794). Fluorescence signals were observed from the $\nu_{1,3}$, $2\nu_2$, and ν_2 vibrational levels of H₂O. Decay of the 2.7 μm , $\nu_{1,3} \rightarrow 0$ fluorescence was a simple single exponential in all mixtures, giving the relaxation rate constants plotted in Figure 2 as a function of HCl mole fraction. The slope and intercept of the least-squares linear fit to the data give the total rate constant $k_{3,HCl}$ for relaxation of H₂O($\nu_{1,3}$) by HCl, which is listed in Table 1.

Attempts were made to observe fluorescence from HCl($\nu=1$) at pressures of 1.2-3.6 Torr in mixtures with $X_{HCl}=0.42$, where ~70% of the relaxation of the H₂O($\nu_{1,3}$) reservoir is by HCl. No fluorescence was observed above the detector noise level. Upper limits of 0.040-0.070 were placed on the ratio of the maximum in the HCl($\nu=1 \rightarrow 0$) fluorescence intensity to the initial fluorescence intensity from the equilibrated ν_1 and ν_3 levels of H₂O. Combined with the radiative lifetimes of the H₂O^{15,20} and HCl²¹ transitions, the measured transmittances of the optical elements over the H₂O and HCl emission bands, and corrections for self-absorption of fluorescence in the flow tube, the results place a conservative upper limit of ~0.032 on the ratio of the maximum in the concentration of HCl($\nu=1$) to the initial concentration of H₂O($\nu_{1,3}$). The experimental upper limit on the concentration ratio and the rate constants for relaxation of H₂O($\nu_{1,3}$) by H₂O,⁴ Ar,² and HCl (Table 1) and for relaxation of HCl by H₂O (Ref. 22 upper limit), Ar,²³ and HCl^{22,24} place an upper limit on the contribution of the intermolecular V→V process in Eq. (10) to the total rate constant for relaxation of H₂O($\nu_{1,3}$) by HCl. Numerical integration of the differential equations for the H₂O($\nu_{1,3}$) and HCl($\nu=1$) level populations determine the conservative *upper limit*, $k_{3V,HCl}/k_{3,HCl} < 0.08$.

Since vibrational transfer from the $\nu_{1,3}$ reservoir to HCl($\nu=1$) is relatively unimportant, the kinetic equations describing the population of the $2\nu_2$ level are simplified. In addition, any

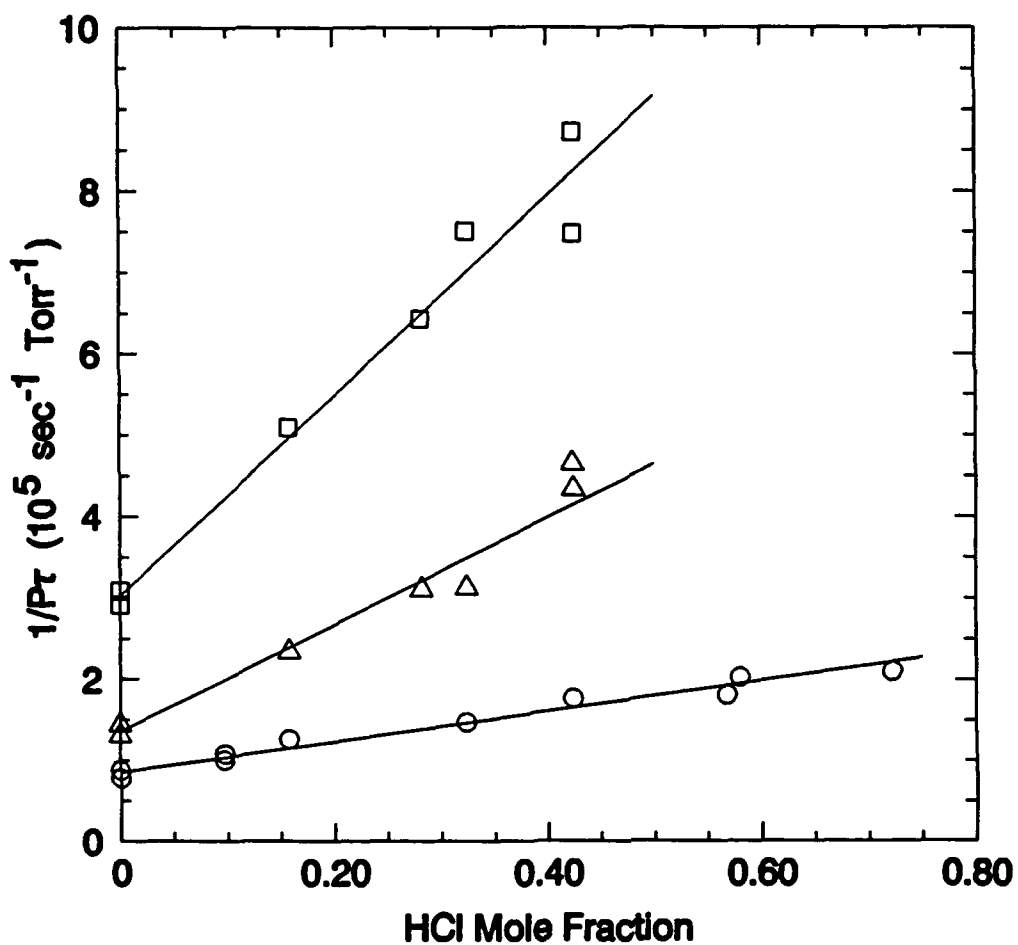


Figure 2. H_2O Vibrational Relaxation in Mixtures of HCl in an $\text{H}_2\text{O}/\text{Ar}$ Carrier Gas. The fixed carrier gas composition was 7.36% H_2O and 92.64% Ar. The observed rate constants are for relaxation of the $\nu_{1,3}$ reservoir (○), ν_2 level (Δ), and $2\nu_2$ level (□). The lines are error-weighted, least-squares linear fits to the data.

contribution from the intermolecular V→V process in Eq. (11) is heavily forward biased (i.e., $k_{2V,HCl}X_{HCl}/k_{2V,HCl}X_{H_2O} > 9$ for $X_{HCl} > 0.15$). Therefore, the solution to the differential equations describing the $H_2O(2\nu_2)$ time-dependent population is essentially the solution given previously for relaxation by a collision partner with no vibrations that participate in the relaxation process. The $6.3\ \mu m$, $2\nu_2 \rightarrow \nu_2$ fluorescence was fit well by a rise/fall double exponential and gave relaxation rate constants for the fluorescence fall equal to those observed from the $2.7\ \mu m$, $\nu_{1,3} \rightarrow 0$ fluorescence decay and rate constants for the fluorescence rise which are plotted in Figure 2. The slope and intercept of the least-squares linear fit to the fluorescence rise data give the total rate constant $k_{2,HCl}$ for relaxation of $H_2O(2\nu_2)$ by HCl, which is listed in Table 1.

An upper limit on the contribution of the intermolecular V→V process in Eq. (11) to the total rate constant for relaxation of $H_2O(2\nu_2)$ by HCl can be estimated from the previously described experimental upper limit on the $HCl(v=1 \rightarrow 0)$ fluorescence intensity from mixtures with $X_{HCl} = 0.42$, where $\sim 78\%$ of the relaxation of the $2\nu_2$ level is by HCl. It is first necessary to establish the fraction of the total rate constant for relaxation of the $\nu_{1,3}$ reservoir which is due to relaxation to the $2\nu_2$ level. For relaxation of $\nu_{1,3}$ by H_2O , we use the experimental lower limit,⁴ $k_{32,H_2O}/k_{3,H_2O} > 0.4$. For relaxation by HCl, the intermolecular V→V relaxation process was shown to be relatively unimportant. For the intramolecular process we use a lower limit, $k_{32,HCl}/k_{3,HCl} > 0.4$, equal to the limit for H_2O self-relaxation. Relaxation by Ar is not significant (i.e., $< 1\%$)² in the gas mixtures used here. The lower limits on $k_{32,M}/k_{3,M}$, the experimental upper limit on the maximum relative concentration of $HCl(v=1)$, and the maximizing assumption, $k_{3V,HCl} \equiv 0$, establish an upper limit on the intermolecular V→V rate constant $k_{2V,HCl}$. The upper limit on $k_{2V,HCl}$ was determined by numerical integration of the differential equations for the $H_2O(\nu_{1,3})$, $H_2O(2\nu_2)$, and $HCl(v=1)$ level populations, using the previously noted experimental upper limit on the maximum in the concentration of $HCl(v=1)$ relative to the initial concentration of $H_2O(\nu_{1,3})$, the rate constants for relaxation of $H_2O(2\nu_2)$ by H_2O ,⁴ Ar,² and HCl (Table 1), and the previously noted rate constants for relaxation of $H_2O(\nu_{1,3})$ and $HCl(v=1)$. The result is the conservative *upper limit*, $k_{2V,HCl}/k_{2,HCl} < 0.16$.

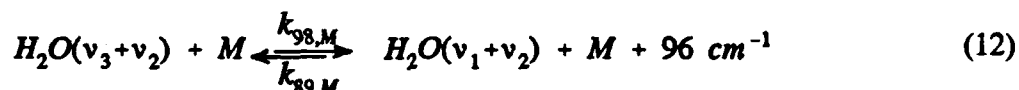
Since energy transfer from both the $\nu_{1,3}$ and $2\nu_2$ levels of H_2O to $HCl(v=1)$ is relatively unimportant, the solutions to the kinetic equations describing the population of the ν_2 vibrational level are essentially those for relaxation of H_2O by a collision partner with no vibrations that participate in the relaxation process. The $6.3\ \mu m$, $2\nu_2 \rightarrow \nu_2$ plus $\nu_2 \rightarrow 0$ fluorescence was fit to a triple exponential with two of the relaxation times fixed at the relaxation times derived from the $\nu_{1,3} \rightarrow 0$ and $2\nu_2 \rightarrow \nu_2$ fluorescence signals for the same gas sample. The observed relaxation rate constants for the ν_2 level are plotted in Figure 2 as a function of HCl mole fraction. The slope and intercept of the least-squares linear fit give the V→T,R rate constant $k_{1,HCl}$, which is listed

in Table 1.

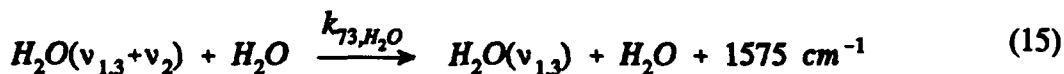
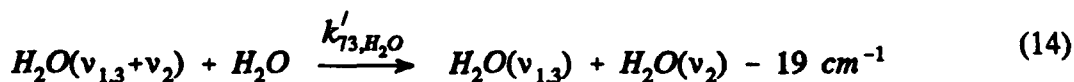
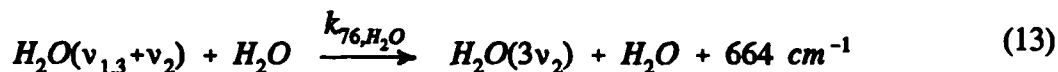
Finally, in the approximation that intermolecular V→V transfer from H₂O to HCl is negligible, the relative amplitudes of the $2\nu_2 \rightarrow \nu_2$ and $\nu_2 \rightarrow 0$ fluorescence signals provide information about path-specific relaxation rate constants through the parameters⁴ $C_{1,\text{HCl}}$ ($\equiv k'_{21,\text{HCl}}$) and Z_{HCl} ($\equiv k'_{31,\text{HCl}}/k_{32,\text{HCl}}$). The results are analogous to those discussed previously for relaxation by H₂. The experimental values were $C_{1,\text{HCl}} = 3.9 \pm 1.1 \times 10^{-11} \text{ cm}^3 \text{ molecule}^{-1} \text{ s}^{-1}$ and $Z_{\text{HCl}} = 0.10 \pm 0.10$. The results imply the rate constant relationships, $k'_{21,\text{HCl}}/k_{2,\text{HCl}} = 0.8 \pm 0.2$ and $k'_{31,\text{HCl}}/k_{32,\text{HCl}} = 0.10 \pm 0.10$. In addition, if it is assumed that $k'_{31,\text{HCl}} > k_{30,\text{HCl}}$, then the value for Z_{HCl} implies $k_{32,\text{HCl}}/k_{3,\text{HCl}} > 0.7$. The derived branching ratios are summarized in Table 2.

C. RELAXATION OF THE $\nu_1 + \nu_2$ AND $\nu_3 + \nu_2$ LEVELS OF H₂O

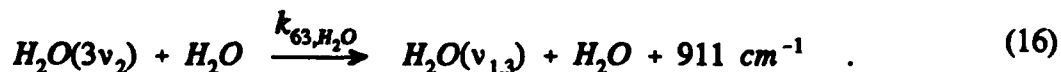
The processes relevant to relaxation of the $\nu_1 + \nu_2$ and $\nu_3 + \nu_2$ combination vibrational levels of H₂O are described in Eqs. (12) through (16). The previous vibrational level numbering system^{1,4} has been extended to include the $3\nu_2$, $\nu_1 + \nu_2$, and $\nu_3 + \nu_2$ levels which are numbered 6, 8, and 9, respectively. Equilibration between the combination levels is described by the process



Relaxation out of the combination levels to the $3\nu_2$ bending overtone level and to the $\nu_{1,3}$ stretching level reservoir is described by the processes



where the notation $\nu_{1,3} + \nu_2$ refers to a reservoir (i.e., "level" 7) of the equilibrated $\nu_1 + \nu_2$ and $\nu_3 + \nu_2$ levels. The rate constants for relaxation of the $\nu_{1,3} + \nu_2$ reservoir are the Boltzmann-weighted averages of the rate constants for relaxation of the two individual combination levels. Finally, relaxation of the $3\nu_2$ level to the stretching reservoir is described by



Energy defects in Eqs. (13) through (16) are given for the $\nu_3 + \nu_2$ initial level and the ν_3 final level where appropriate.¹⁸ The rate constants in Eqs. (14) through (16) are the sum of the rate constants for relaxation to the two individual final stretching levels. The path-specific relaxation processes in Eqs. (12) through (16) are not the complete set, but are sufficient for the present discussion. We also define $k_{6,M}$ and $k_{7,M}$ as the total relaxation rate constants (i.e., the sum over the complete set of path-specific rate constants) for the $3\nu_2$ level and the $\nu_{1,3} + \nu_2$ reservoir, respectively.

Vibrational relaxation of the stretch-plus-bend combination levels was investigated in H_2O/Ar mixtures, following direct laser excitation to the $H_2O(\nu_3 + \nu_2)$ level. Fluorescence was observed on the $2.7\ \mu m$, $\nu_3 + \nu_2 \rightarrow \nu_2$ hot band through an H_2O cold gas filter. Fluorescence on the $\nu_3 \rightarrow 0$ fundamental band was obtained by subtracting the signal observed through the H_2O -pressurized, cold gas filter from the signal observed through an evacuated filter for the same gas sample. Fluorescence at $2.7\ \mu m$ on the $\nu_1 + \nu_2 \rightarrow \nu_2$ and $\nu_1 \rightarrow 0$ transitions is expected to be very weak because of the much smaller band strength of the transitions (i.e., factor of $15\text{--}20$ ^{15,20}). The $\nu_3 + \nu_2 \rightarrow \nu_2$ fluorescence signal was found to be a fast, single exponential decay with a low intensity, slowly decaying tail attributed to a small leakage of $\nu_3 \rightarrow 0$ (and $\nu_1 \rightarrow 0$) fluorescence through the cold gas filter. The peak amplitude of the slow tail was only 5-10% of the peak amplitude of the $\nu_3 + \nu_2 \rightarrow \nu_2$ fluorescence, and the slow decay time was identical to the slow decay time of the $\nu_3 \rightarrow 0$ fluorescence signal. The $\nu_3 \rightarrow 0$ fluorescence signal was found to have a fast rise time similar to the fast decay time of the $\nu_3 + \nu_2 \rightarrow \nu_2$ fluorescence, followed by a much slower single exponential decay. The relaxation rate constant of the fast $\nu_3 + \nu_2 \rightarrow \nu_2$ fluorescence decay and the rate constant of the slow $\nu_3 \rightarrow 0$ fluorescence decay are plotted in Figure 3 as a function of the mole fraction of H_2O in Ar . The slope and intercept of the least-squares linear fit to the $\nu_3 + \nu_2 \rightarrow \nu_2$ fluorescence decay data give the value listed in Table 1 as the total rate constant k_{7,H_2O} for relaxation of the $\nu_{1,3} + \nu_2$ reservoir by H_2O and the upper limit listed for $k_{7,Ar}$. The fit to the slow $\nu_3 \rightarrow 0$ fluorescence decay data gives a rate constant for relaxation by H_2O which is identical ($\pm 2\%$) to the rate constant k_{3,H_2O} for relaxation of the $\nu_{1,3}$ reservoir determined previously by direct excitation of $H_2O(\nu_3)$.⁴ Low signal-to-noise precluded any detailed investigation of the initial, rapid equilibration between the $\nu_1 + \nu_2$ and $\nu_3 + \nu_2$ levels either by direct laser excitation of $\nu_1 + \nu_2$, or by the use of very low sample pressures.

We interpret the rate constant measured here for relaxation of the $\nu_3 + \nu_2 \rightarrow \nu_2$ fluorescence as the rate constant for relaxation of a reservoir consisting of the equilibrated $\nu_1 + \nu_2$ and $\nu_3 + \nu_2$ vibrational levels. By analogy with relaxation of the ν_1 and ν_3 stretching levels, it is likely that equilibration between the nearly resonant, Coriolis-coupled $\nu_1 + \nu_2$ and $\nu_3 + \nu_2$ combination levels is faster than relaxation out of the two levels to other states. The lower limit on the rate constant for equilibration between the ν_1 and ν_3 levels in H_2O/H_2O collisions¹ is a factor of 2 faster than the rate constant measured here for relaxation of the $\nu_3 + \nu_2 \rightarrow \nu_2$ fluorescence by H_2O .

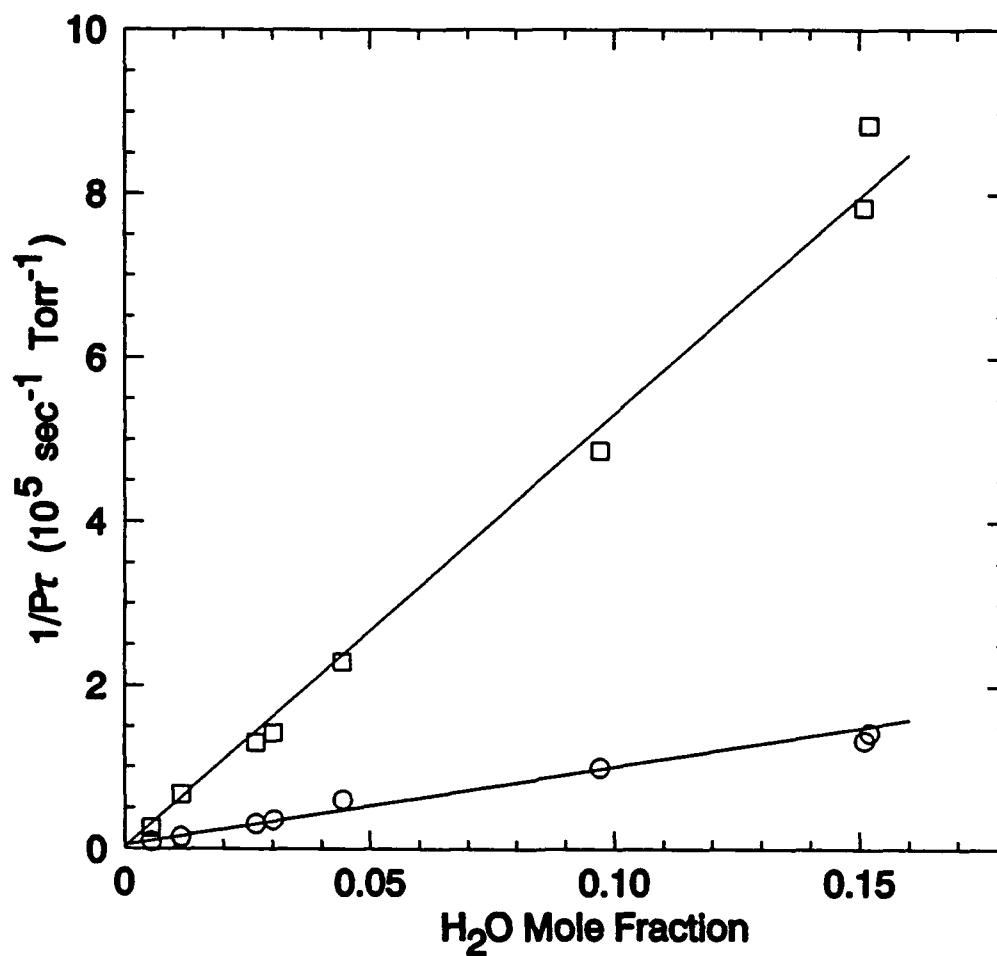


Figure 3. H₂O Vibrational Relaxation in H₂O/Ar Mixtures. The observed rate constants are for relaxation of the $\nu_{1,3} + \nu_2$ (□) and $\nu_{1,3}$ (○) reservoirs. The lines are error-weighted, least-squares linear fits to the data.

Also, if equilibration between $\nu_1 + \nu_2$ and $\nu_3 + \nu_2$ requires only a few collisions with Ar as theory indicates for the fundamental stretching levels,¹⁷ then equilibration due to collisions with Ar would be several times faster than the $\nu_3 + \nu_2 \rightarrow \nu_2$ fluorescence relaxation rates measured at the low mole fractions of H₂O used in these experiments. It should be noted that if equilibration between the combination levels is not faster than the observed relaxation rate of the $\nu_3 + \nu_2 \rightarrow \nu_2$ fluorescence, then the observed relaxation rate can be interpreted as either the rate for relaxation of $\nu_3 + \nu_2$ to levels other than $\nu_1 + \nu_2$, or a lower limit on the rate for relaxation of $\nu_1 + \nu_2$ to levels other than $\nu_3 + \nu_2$.

Assuming that the two combination levels relax in equilibrium, the relative intensities of the $\nu_3 \rightarrow 0$ and $\nu_3 + \nu_2 \rightarrow \nu_2$ fluorescence signals can be used to determine the fraction of the rate constant for relaxation of the $\nu_{1,3} + \nu_2$ reservoir by H₂O which is due to direct, one-step relaxation to the $\nu_{1,3}$ reservoir. For self-relaxation the ratio of the time-integrated fluorescence intensities is given by

$$\frac{\int_0^\infty I_{\nu_3 \rightarrow 0}(t) dt}{\int_0^\infty I_{\nu_3 + \nu_2 \rightarrow \nu_2}(t) dt} = \frac{\tau_{R, \nu_3 + \nu_2 \rightarrow \nu_2} k_{7, H_2O}}{\tau_{R, \nu_3 \rightarrow 0} k_{3, H_2O}} \left[\frac{k_{76, H_2O} k_{63, H_2O}}{k_{7, H_2O} k_{6, H_2O}} + \frac{k'_{73, H_2O} + k_{73, H_2O}}{k_{7, H_2O}} \right] \quad (17)$$

The radiative lifetimes τ_R on the hot band and fundamental band are assumed to be equal, using the harmonic oscillator approximation. The experimental value for the ratio of the integrated fluorescence intensities was 1.5 ± 0.4 for H₂O mole fractions greater than 0.01, where relaxation was entirely (>99%) by H₂O. The integrated fluorescence ratio implies the upper limit, $0.40 > (k'_{73, H_2O} + k_{73, H_2O})/k_{7, H_2O}$. Thus, less than 40% of the total relaxation rate constant is due to relaxation directly to the $\nu_{1,3}$ reservoir. Conversely, more than 60% of the total relaxation rate constant is due to relaxation to final states involving only the bending mode and the ground level.

IV. DISCUSSION

Vibrational relaxation of H_2O by HCl is very similar to relaxation by H_2O itself. The probabilities per collision for relaxation of the $\nu_{1,3}$ stretching reservoir, the $2\nu_2$ level, and the ν_2 level by HCl are large and differ from the H_2O self-relaxation probabilities by factors of only 3.6, 2.7, and 2.2, respectively. The dominant paths for relaxation of the $\text{H}_2\text{O}(\nu_{1,3})$ stretching reservoir are similar for the two collision partners. Intermolecular $\text{V} \rightarrow \text{V}$ relaxation of the $\nu_{1,3}$ reservoir by H_2O itself (i.e., Eq. (8)) and by HCl (i.e., Eq. (10)) is a minor factor compared to intramolecular relaxation to the $2\nu_2$ level, which proceeds with roughly the same exothermicity (i.e., Eq. (1)). As the results in Table 2 indicate, the intramolecular path is several times more efficient than the intermolecular path for both collision partners (i.e., $k_{32,\text{HCl}}/k_{3\text{V},\text{HCl}} > 7$ and $k_{32,\text{H}_2\text{O}}/k_{31,\text{H}_2\text{O}} > 5$). It is noted that the $\nu_{1,3} \rightarrow 2\nu_2$ self-relaxation process in Eq. (8) may in principle be either intramolecular, or intermolecular; however, the intramolecular process seems the least complicated and most likely. Another more striking similarity between the H_2O and HCl collision partners is found in the relaxation of the $\text{H}_2\text{O}(2\nu_2)$ vibrational level. Nearly resonant, intermolecular, $\text{V} \rightarrow \text{V}$ relaxation of the $2\nu_2$ level by H_2O itself (i.e., Eq. (9)) and by HCl (i.e., Eq. (11)) is surprisingly not the major relaxation path. In both cases the near resonant intermolecular path accounts for at most a small fraction of the total relaxation rate constant (i.e., $k_{2\text{V},\text{HCl}}/k_{2,\text{HCl}} < 0.15$ and $k_{21,\text{H}_2\text{O}}/k_{2,\text{H}_2\text{O}} < 0.3$). Relaxation of the $2\nu_2$ level by both collision partners is dominated by the much more exothermic $\text{V} \rightarrow \text{T,R}$ relaxation of a single bending quantum (i.e., Eq. (4)).

The similarity of the relaxation probabilities and dominant paths for relaxation of H_2O by H_2O and HCl are presumably the result of similar collision dynamics. H_2O and HCl are strong to moderate hydrogen bonding molecules with heats of dimerization of ~ 6 kcal/mol and ~ 2 kcal/mol, respectively.^{13,25} The dominant influence of the attractive part of the intermolecular potential is seen in the large magnitude and negative temperature dependence of the self-relaxation probabilities of both molecules near room temperature and below.^{2,4,24} The importance of rotational motion has also been demonstrated in deuteration studies of the self-relaxation of both molecules.^{3,22} Assuming that the attractive forces between H_2O and HCl are similar in strength and rotational anisotropy to those of the $\text{H}_2\text{O}/\text{H}_2\text{O}$ and HCl/HCl interactions, one would expect attraction and rotational motion to dominate the relaxation of H_2O by HCl . It is also likely that the temperature dependencies of the probabilities for relaxation of H_2O by HCl and other hydrogen halides are qualitatively similar to those for H_2O self-relaxation.

The relative unimportance of intermolecular $\text{V} \rightarrow \text{V}$ processes in the relaxation of the $\nu_{1,3}$ and $2\nu_2$ levels of H_2O by H_2O and HCl is probably the result of the extraordinary efficiency of competing intramolecular and $\text{V} \rightarrow \text{T,R}$ paths, rather than anomalously small probabilities for intermolecular $\text{V} \rightarrow \text{V}$ transfer. By analogy with single quantum, intermolecular $\text{V} \rightarrow \text{V}$ energy

transfer probabilities in the strongly hydrogen bonding HF molecule^{26,27} and other hydrogen halides,^{28,29} it seems likely that the intermolecular V→V processes for relaxation of H₂O by H₂O and HCl require at least 10-100 collisions for exothermicities of 0-500 cm⁻¹. By these rough estimates the intermolecular V→V probabilities would be large, but nevertheless significantly smaller than the measured total relaxation probabilities for the $\nu_{1,3}$ and $2\nu_2$ levels of H₂O. Relaxation of the $\nu_{1,3}$ level by H₂O and HCl is dominated by efficient intramolecular V→V relaxation to the $2\nu_2$ level. The ν_3 and $2\nu_2$ vibrational levels of H₂O are Coriolis-coupled and the ν_1 and $2\nu_2$ levels are Fermi-coupled in the isolated molecule with large mixing coefficients for some rotational states.³⁰ The relaxation data suggest that collisions with strong rotational anisotropy and/or strong attractive forces mix the triad of vibrational states very efficiently leading to rapid intramolecular relaxation of the stretching levels to the bending overtone level, as well as extremely rapid relaxation between the Coriolis-coupled ν_1 and ν_3 stretching levels.¹ Relaxation of the $2\nu_2$ level by H₂O and HCl is dominated by V→T,R relaxation to the ν_2 level. The extraordinary magnitude of the probability for V→T,R self-relaxation of the H₂O bending vibration has been explained by theories which include the effects of the strong attractive potential and rotational motion.^{12,13} It is likely that the same factors contribute to rapid V→T,R relaxation of H₂O bending motion by HCl.

Vibrational relaxation of H₂O by H₂ is 1-2 orders of magnitude less efficient than relaxation by H₂O or HCl. The lower efficiency of H₂ probably reflects the absence of strong attractive forces between H₂ and H₂O. Relaxation by H₂ may be induced primarily by the repulsive part of the intermolecular potential. Some data for the relaxation of H₂O by molecules which do not hydrogen bond are available for comparison with the H₂ results. The probability per hard sphere collision for relaxation of the H₂O($\nu_{1,3}$) reservoir by H₂ is approximately the same as the probabilities measured for relaxation by N₂ and O₂, and is approximately an order of magnitude larger than the probability for relaxation by He.² Considering the inefficiency of intermolecular V→V transfer from H₂O, it seems likely that relaxation by N₂ and O₂ is predominantly intramolecular, as the experiments indicate is the case for relaxation by H₂. Therefore, the three diatomic molecules must have similar efficiencies for collisionally mixing the H₂O stretching and bending overtone levels and removing the exothermicity of the relaxation process, presumably to some extent through the diatomic rotational degree of freedom. The probability for single bending quantum, V→T,R relaxation of the $2\nu_2$ level is a factor of ~6 larger for H₂ than for relaxation by He.² In simple, repulsive-potential, energy transfer theories, the larger probability for H₂ can reflect both the higher translational speed of H₂ and the participation of H₂ rotational motion in the relaxation process. A comparison of the probabilities for relaxation of D₂O(ν_2) by D₂ and He has suggested that the rotation of D₂ participates significantly in V→T,R relaxation of the water bending vibration.³ The same is probably true for relaxation of the $2\nu_2$ and ν_2 levels of H₂O by H₂.

The rate constant for relaxation of the H₂O($\nu_{1,3} + \nu_2$) combination level reservoir by H₂O

is nearly gas kinetic. Direct relaxation to the $\nu_{1,3}$ stretching reservoir through intermolecular V \rightarrow V transfer of a bending quantum (i.e., Eq. (14)) and V \rightarrow T,R relaxation of a bending quantum (i.e., Eq. (15)) is demonstrated experimentally to account for < 40% of the rate constant. The result is consistent with very rough estimates of the rate constants for the bending quantum V \rightarrow V transfer and V \rightarrow T,R relaxation processes, based on the self-relaxation rate constants for the analogous processes in Eqs. (9) and (6), respectively. The dominant path (> 60%) for relaxation of the combination levels is to final states involving only pure bending levels and the ground level. Assuming intermolecular V \rightarrow V processes are relatively inefficient, the most likely relaxation process would seem to be intramolecular relaxation of the combination levels to the $3\nu_2$ bending overtone. The $\nu_1 + \nu_2$, $\nu_3 + \nu_2$, and $3\nu_2$ levels of H₂O are mixed by Coriolis and Fermi interactions in the isolated molecule.³¹ The mixing coefficients are similar to those for the lower energy triad of levels $\{\nu_1, \nu_3, 2\nu_2\}$.

The rate constant for relaxation of the $\nu_{1,3} + \nu_2$ combination level reservoir to the manifold of bending levels is several times faster than the rate constant for the analogous relaxation of the $\nu_{1,3}$ stretching reservoir to the bending manifold. The latter rate constant is also slower than the rate constants for V \rightarrow T,R equilibration among the bending levels. The result suggests that the combination levels communicate more efficiently with the bending levels and hence with translation and rotation than do the fundamental stretching levels. In some nonequilibrium situations, the $\nu_{1,3} + \nu_2$ reservoir, and perhaps higher combination levels involving the stretching vibrations, may be characterized by vibrational temperatures more closely aligned with the bending mode vibrational temperature and the translational/rotational temperature than with the vibrational temperature of the fundamental stretching levels.

REFERENCES

1. J. Finzi, F.E. Hovis, V.N. Panfilov, P. Hess and C.B. Moore, *J. Chem. Phys.* **67**, 4053 (1977).
2. F.E. Hovis and C.B. Moore, *J. Chem. Phys.* **72**, 2397 (1980).
3. S.S. Miljanic and C.B. Moore, *J. Chem. Phys.* **73**, 226 (1980).
4. P.F. Zittel and D.E. Masturzo, *J. Chem. Phys.* **90**, 977 (1989).
5. R.L. Sheffield, K. Boyer and A. Javan, *Opt. Lett.* **5**, 10 (1980).
6. A. Hariri and C. Wittig, *J. Chem. Phys.* **68**, 2109 (1978).
7. A.J. Grimley and P.L. Houston, *J. Chem. Phys.* **69**, 2339 (1978).
8. R.G. Keeton and H.E. Bass, *J. Acoust. Soc. Am.* **60**, 78 (1976), and references therein.
9. H.E. Bass, R.G. Keeton and D. Williams, *J. Acoust. Soc. Am.* **60**, 74 (1976).
10. R.T.V. Kung and R.E. Center, *J. Chem. Phys.* **62**, 2187 (1975).
11. W.J. Sarjeant, Z. Kucеровsky and E. Brannen, *Appl. Opt.* **11**, 735 (1972).
12. S.S. Miljanic, *J. Chem. Soc. Faraday Trans. 2* **81**, 517 (1985); **80**, 275 (1984).
13. H.K. Shin, *J. Chem. Phys.* **69**, 1240 (1978).
14. J. Ree and H.K. Shin, *Chem. Phys. Lett.* **167**, 220 (1990); *J. Chem. Phys.* **93**, 6463 (1990).
15. J.M. Flaud and C. Camy-Peyret, *J. Mol. Spectrosc.* **55**, 278 (1975).
16. C. Camy-Peyret, J.M. Flaud and R.A. Toth, *J. Mol. Spectrosc.* **67**, 117 (1977).
17. J. Ree and H.K. Shin, *Chem. Phys. Lett.* **163**, 308 (1989).
18. L.A. Pugh and K.N. Rao, *J. Mol. Spectrosc.* **47**, 403 (1973).
19. V.L. Orkin, *Kinet. Katal.* **23**, 315 (1982).
20. R.A. Toth, *J. Quant. Spectrosc. Radiat. Transfer* **13**, 1127 (1973).
21. R.A. Toth, R.H. Hunt and E.K. Plyler, *J. Mol. Spectrosc.* **35**, 110 (1970).
22. H.-L. Chen and C.B. Moore, *J. Chem. Phys.* **54**, 4072 (1971).
23. R.V. Steele, Jr. and C.B. Moore, *J. Chem. Phys.* **60**, 2794 (1974).
24. P.F. Zittel and C.B. Moore, *J. Chem. Phys.* **59**, 6636 (1973).
25. D.H. Rank, P. Sitaram, W.A. Glickman, and T.A. Wiggins, *J. Chem. Phys.* **39**, 2673 (1963).
26. J.M. Robinson, D.J. Pearson, R.A. Copeland, and F.F. Crim, *J. Chem. Phys.* **82**, 780 (1985); J.M. Robinson, K.J. Rensberger, and F.F. Crim, *ibid.* **84**, 220 (1986).
27. L.S. Dzelzkalns and F. Kaufman, *J. Chem. Phys.* **79**, 3363 (1983).

28. A.B. Horwitz and S.R. Leone, *J. Chem. Phys.* **69**, 5319 (1978).
29. C.J. Dasch and C.B. Moore, *J. Chem. Phys.* **72**, 4117 (1980).
30. J.M. Flaud and C. Camy-Peyret, *J. Mol. Spectrosc.* **51**, 142 (1974).
31. C. Camy-Peyret and J.M. Flaud, *J. Mol. Spectrosc.* **59**, 327 (1976).